Expression and Localization of Bestrophin during Normal Mouse Development

Benjamin Bakall,[1] *Lihua Y. Marmorstein,*[2] *George Hoppe,*[2] *Neal S. Peachey,*[2,3] *Claes Wadelius,*[1] *and Alan D. Marmorstein*[2,4]

Purpose. Best macular dystrophy is caused by mutations in the *VMD2* gene, which encodes the protein bestrophin. The purpose of this study was to determine the postnatal onset of expression of bestrophin mRNA and protein in the mouse retinal pigment epithelium (RPE).

Methods. Rabbit anti-mouse bestrophin polyclonal antisera designated Pab-003 was generated against a peptide derived from the C terminus of mouse bestrophin and characterized by Western blot and immunofluorescence staining of transfected cells. Expression of bestrophin mRNA during ocular development was studied with quantitative PCR. Bestrophin protein expression in the developing eye was observed by using immunohistochemistry. The onset of mouse phototransduction was determined by conventional electroretinography (ERG).

Results. Bestrophin mRNA was detected at embryonic day 15 in whole mouse eyes by RT-PCR. Real-time quantification of mouse bestrophin mRNA levels indicated that the highest levels of mRNA were present in the early postnatal period. In contrast, bestrophin in the RPE was first detected at postnatal day (P)10 by immunohistochemistry. Phototransduction, as determined by the presence of an ERG a-wave, was first observed at P10.

Conclusions. The results of this study show that mouse bestrophin mRNA is present in the eye during embryogenesis and significantly precedes the onset of bestrophin protein expression at P10. The appearance of bestrophin in the basolateral plasma membrane of the RPE is coincident with the first detectable ERG a-wave. Because bestrophin is thought to play a role in generating the light peak, a late response of the ERG, these data support a temporal role for bestrophin in RPE responses to light. Furthermore, bestrophin protein appears to be a very late marker of RPE differentiation and to be subject to strong translational control. (*Invest Ophthalmol Vis Sci.* 2003; 44:3622–3628) DOI:10.1167/iovs.03-0030

From the [1]Department of Genetics and Pathology, Rudbeck Laboratory, Uppsala University, Uppsala, Sweden; the [2]Department of Ophthalmic Research, Cole Eye Institute, Cleveland Clinic Foundation, Cleveland, Ohio; the [3]Research Service, Cleveland Veterans Administration Medical Center, Cleveland, Ohio; and the [4]Department of Cell Biology, Lerner Research Institute, Cleveland Clinic Foundation, Cleveland, Ohio.

Supported by National Eye Institute Grants EY13160 (ADM) and EY13847 (LYM), the Veterans Administration (NSP), the Swedish Research Council (CW, BB), the Synfrämjandets Research Foundation (BB), the Swedish Society for Medical Research (BB), and the Markus Borgstrom Foundation (CW).

Submitted for publication January 13, 2003; revised February 18, 2003; accepted March 18, 2003.

Disclosure: **B. Bakall**, Merck & Co., Inc. (P); **L.Y. Marmorstein**, None; **G. Hoppe**, None; **N.S. Peachey**, None; **C. Wadelius**, Merck & Co., Inc. (P); **A.D. Marmorstein**, None

The publication costs of this article were defrayed in part by page charge payment. This article must therefore be marked "*advertisement*" in accordance with 18 U.S.C. §1734 solely to indicate this fact.

Corresponding author: Alan D. Marmorstein, Cole Eye Institute, i31, Cleveland Clinic Foundation, 9500 Euclid Avenue, Cleveland, OH 44195; marmora@ccf.org.

Best macular dystrophy (BMD; OMIM 153700; www.ncbi.nlm.nih.gov/Omim; Online Mendelian Inheritance in Man, provided in the public domain by the National Center for Biotechnology, Bethesda, MD), also called vitelliform macular dystrophy, is an autosomal dominant inherited disease characterized by early-onset macular degeneration. The gene causing BMD, *VMD2*, is located on chromosome 11 (at q13).[1,2] To date, more than 80 mutations have been reported in the *VMD2* gene in patients with BMD,[1–12] a summary of which can be found in the *VMD2* mutation database (www.uni-wuerzburg.de/humangenetics/vmd2.html).

Diagnosis of BMD typically is made after the finding of a vitelliform or egg yolk lesion in the macula that can be observed by fundus examination.[13,14] However, before identification of the *VMD2* gene, conclusive diagnosis of BMD in patients with vitelliform lesions was based on the finding of an abnormal electrooculogram (EOG), without aberrations in the clinical electroretinogram (ERG).[13,14] It has been shown that individuals with BMD exhibit an altered EOG, even before any abnormalities can be observed by fundus examination.[15,16] The EOG records the same response, termed the light peak, that can be recorded using DC amplification of the ERG (the DC-ERG). DC-ERG studies on chick retina-RPE-choroid preparations have shown that the light peak is generated by a depolarization of the basal plasma membrane of the RPE[17] due to activation of a chloride conductance.[17–19] Studies on Cl^--coupled H_2O transport by the RPE suggest that the Cl^- conductance is Ca^{2+} sensitive.[17] Recently, Sun et al.[20] have suggested that bestrophin functions as a Ca^{2+} dependent Cl^- channel. We have produced antibodies that recognize human bestrophin and demonstrated that it is localized to the basolateral plasma membrane of RPE cells,[21] consistent with a role for bestrophin in the generation or regulation of the EOG light peak. The light peak is thought to be stimulated by an as yet unidentified photoreceptor-derived chemical messenger and transduced across the RPE cell through a signal transduction pathway. We have recently shown[22] that bestrophin physically interacts with the serine/threonine protein phosphatase PP2A, that bestrophin is phosphorylated, and that bestrophin phosphorylation is sensitive to PP2A activity, suggesting its participation in a signal transduction pathway.

The mouse has been a crucial animal model for the study of retinal genes and eye disease. To develop a body of information regarding mouse bestrophin, we isolated and cloned the mouse bestrophin cDNA, analyzed the expression of the mouse bestrophin mRNA and protein, and determined the localization of mouse bestrophin protein during normal development. Our findings indicate that, despite early expression of bestrophin mRNA, expression of bestrophin protein occurs very late in postnatal development. This time point matches the onset of light-evoked electrical responses in the outer retina, and the results support a role for bestrophin in the RPE response to ionic changes that accompany retinal activity.

Materials and Methods

Computer Analysis

Pair-wise global alignments with Blosum62 were performed, using the needle program with Needleman-Wunsch algorithm from the Emboss

Investigative Ophthalmology & Visual Science, August 2003, Vol. 44, No. 8

package (http://www.no.embnet.org/ Biotechnology Center of Oslo, University of Oslo, Oslo, Norway). Prediction of mouse bestrophin topology and transmembrane was predicted using a consensus from the following programs: HMTOP (http://www.enzim.hu/hmmtop/ Institute of Enzymology, Budapest, Hungary), TMHMM 2.0 (http://www.cbs.dtu.dk/services/TMHMM-2.0/ Center for Biological Sequence Analysis, Technical University of Denmark, Lyngby, Denmark), SOSUI (sosui.proteome.bio.tuat.ac.jp/sosuiframe0.html/ Mitaku Laboratory, Department of Biotechnology, Tokyo University of Agriculture and Technology, Tokyo, Japan), DAS (www.sbc.su.se/~miklos/DAS/ Stockholm Bioinformatics, Center, Stockholm, University, Stockholm Sweden), and TOPPRED (bioweb.pasteur.fr/seqanal/interfaces/toppred.html/ The Pasteur Institute, Paris, France). All databases are provided in the public domain.

Tissue Samples and RNA Extraction

All animals were handled according to the ARVO Statement for the Use of Animals in Ophthalmic and Vision Research. BALBc mice for RT-PCR and *Taq* polymerase analysis (*Taq*Man) were obtained from M&B (Ry, Denmark) and from Harlan (Indianapolis, IN) for immunohistochemistry and electroretinography. Beginning at embryonic day (E)15, mice were killed and eyes enucleated. For RNA extraction, eyes were immediately frozen and stored at −80°C. Whole eyes from each developmental stage were homogenized in 0.5 mL extraction reagent (TRIzol; Invitrogen, Carlsbad, CA) according to the manufacturer's protocol.

Reverse Transcription–Polymerase Chain Reaction

Target RNA (1 μg) was reverse transcribed with a commercial system (Superscript First-Strand Synthesis System for RT-PCR; Invitrogen). This process yielded 20 μL cDNA, of which 2 μL was used to PCR amplify a 617-bp bestrophin fragment. The following primers were used: 5′-TACACAGCTGCTTCTGCCAG-3′ (forward), 5′-TCACTCATAGAGAACAGGTTTGGTGC-3′ (reverse). PCR products were visualized on an ethidium bromide–stained agarose gel.

Cloning Mouse Bestrophin cDNA

The mouse bestrophin cDNA was amplified from mouse testis cDNA (Clontech, Palo Alto, CA) by PCR using DNA polymerase (DeepVent; New England Biolabs, Beverly, MA) and PCR primers corresponding to the 20 bases in the 5′ and 3′ ends of the coding region of the cDNA sequence assembled from the Celera database (accession no. mCG1951).[22] It has been reported that bestrophin mRNA is present in testis.[1,2,23] The 1653 bp coding sequence was subcloned either into pcDNA3.1 (pcDNA3.1-mbest) or, to generate a fusion protein with green fluorescent protein (GFP), the mouse bestrophin cDNA was cloned in-frame into pEGFP-N1 (pEGFP-mbest).

Real-Time PCR

Primers and probes were generated on computer (Primer Express software; Applied Biosystems, Foster City, CA). To avoid spurious amplification of genomic DNA, PCR products were designed that spanned at least two exons. The predicted amplification product sizes for bestrophin and GAPDH were 130 and 238 bp, respectively. FAM- and TAMRA-labeled probes were purchased from Applied Biosystems. The plasmid pEGFP-N1-mbest was used as a quantitative standard to estimate bestrophin expression. Real-time PCR was performed with a PCR kit and sequence detector (*Taq*Man PCR Kit in a model 7700 Sequence Detector; Applied Biosystems). The reaction conditions were 50°C for 2 minutes, 95°C for 10 minutes, and 40 cycles of 95°C for 15 seconds and 57.5°C for 1 minute. Total RNA (1 μg) from whole mouse eyes was reverse transcribed using a RT-PCR kit (Superscript First-Strand Synthesis System; Invitrogen), yielding 20 μL cDNA. For each quantitative PCR reaction for mouse bestrophin, 1 μL cDNA was used as a template, and for mouse GAPDH, 0.25 μL of template was used. The template was mixed with 3.5 mM $MgCl_2$; 200 μM each of dATP, dCTP, and dGTP; 400 μM dUTP; 0.025 U/μL polymerase (AmpliTaq Gold; Applied Biosystems), and a 25-nM probe (*Taq*Man; Applied Biosystems) for bestrophin or a 33-nM probe for GAPDH. Each bestrophin reaction was performed in triplicate, and each GAPDH reaction was performed in duplicate in the same plate. The mRNA expression levels of bestrophin were calculated as relative mRNA expression rates. Mouse bestrophin and GAPDH cDNAs were estimated, with a standard curve representing the log of the input amount. Rates of bestrophin mRNA expression were normalized to that of GAPDH.

Primers and *Taq* probes used for real-time PCR: bestrophin, 5′-CTGCTTCTGCCAGGTCTCG-3′ (forward) and 5′- TCCGTGTCAGCCTCCTCTTTT-3′ (reverse) with FAM-CTCCACCTTCAACATCAGCCTAAAGAAAGAAGAC-TAMRA (bestrophin probe); GAPDH: 5′-CTTCACCACCATggAgAAggC-3′ (forward) and 5′-ggCATggACTgTggTCATgAg-3′ (reverse) with FAM-CCTGGCCAAGGTCATCCATGACAACTTT-TAMRA (GAPDH probe).

Antibody Production

A polyclonal antiserum was produced as described previously[21] in New Zealand White rabbits immunized with the peptide AESYPYRDEAGTKPVLYE coupled to keyhole limpet hemocyanin by the glutaraldehyde cross-linking method.[24] All experiments were performed using the total IgG fraction, which we refer to herein as Pab-003.

Cell Culture and Western Blot

RPE-J cells were maintained in DMEM supplemented with 4% FBS, nonessential amino acids, glutamine, and penicillin-streptomycin at 32°C in a 5% CO_2 incubator, as previously described.[23]

For Western blot experiments, RPE-J cells grown in 35-mm plates to 80% confluence were transfected with pEGFP-N1, pcDNA3.1-mbest, or pEGFP-N1-mbest, with a lipophilic transfection reagent (Lipofectamine; Invitrogen), as described previously.[25] Western blot analysis were performed as described previously,[21,25–27] by using alkaline-phosphatase–conjugated secondary antibodies and nitroblue tetrazolium/5-bromo-4-chloro-3-inodyl phosphate (NBT-BCIP), or horseradish peroxide–conjugated secondary antibodies and enhanced chemiluminescence (ECL+; Amersham, Amersham, UK).

Immunofluorescence

For immunofluorescence, RPE-J cells grown on poly-D-lysine–coated (BD Biosciences Discovery Labware, Bedford, MA) coverslips were transfected using the transfection reagent (Lipofectamine; Invitrogen) as described previously.[21,28] After 48 hours, cells were fixed in −20°C methanol and stained for mouse bestrophin using 1 μg/mL Pab-003 as the primary antibody and Texas red–conjugated goat-anti-rabbit IgG as the secondary antibody. Nuclei were stained with 4′,6-diamino-2-phenylindole (DAPI). The cells were examined by microscope (Microphot-2; Nikon, Tokyo, Japan). Images were acquired with a cooled CCD camera and accompanying software (SPOT-2 camera, MetaMorph ver. 4.5 software; Universal Imaging, Media, PA) and processed on computer (PhotoShop version 5.5; Adobe Systems, Mountain View, CA).

Immunocytochemistry

Immunohistochemistry was performed as before.[21,28] In brief, eyes were enucleated and immediately placed in 4% paraformaldehyde in PBS for 24 to 72 hours. Tissues were processed for paraffin embedding and cut in 8-μm sections. Sections were deparaffinized with xylene, hydrated through graded ethanols, and subjected to pressurized heat-mediated antigen retrieval in 0.01 M sodium citrate (pH 6.0), at 121°C for 1.5 minutes. Tissue sections were incubated with 3% BSA in 0.1 M phosphate buffer (pH 7.2), for 30 minutes, then incubated overnight at 4°C with Pab-003. After the sections were washed with PBS, they were further processed with an avidin-biotin complex kit (ABC kit; Vector Laboratories, Burlingame, CA) with 3,3′-diaminobenzidine as substrate.

After counterstaining with nuclear fast red, sections were viewed and images captured, as described for immunofluorescence.

Electroretinography

After overnight dark adaptation, mice were anesthetized with ketamine (40 mg/kg) and xylazine (8 mg/kg). The eyelids of the left eyes were then excised with a scissors and topical anesthetic (1% proparacaine HCl) was applied. The pupil was dilated with eye drops (1% tropicamide; 2.5% phenylephrine HCl; 1% cyclopentolate), and the mouse was placed on a heating pad. The ERG was recorded using a thin stainless steel wire contacting the corneal surface through a layer of 1% methylcellulose. Platinum needle electrodes placed in the cheek below the test eye and tail served as reference and ground leads, respectively. The signal was differentially amplified (band-pass filter of 0.05–1000 Hz), digitized at 1000 Hz, and stored using a visual electrodiagnostic system (UTAS E-3000; LKC, Gaithersburg, MD).

Recording sessions were designed to be brief. From each mouse, a dark-adapted response series was recorded using strobe flash stimuli presented in a Ganzfeld (LKC), that ranged in intensity from −0.8 to +0.9 log cd-sec/m^2. Stimuli were presented in order of increasing intensity, and responses to 25 successive flashes were averaged, with a 5.1-second interflash interval. The amplitudes of the a-wave and of slow PIII were measured from the prestimulus baseline to the trough of the a-wave or of slow PIII, respectively. When present, the amplitude of the b-wave was measured from the a-wave trough to the b-wave peak.

Results

The cDNA sequence of mouse bestrophin was deduced from the Celera database (Celera, Rockville, MD) entry as previously described.[22] We obtained a full-length cDNA for mouse bestrophin by RT-PCR from a mouse testis cDNA library, using primers matching the 5′ and 3′ regions of the predicted open reading frame. DNA sequence analysis of the PCR product confirmed the predicted sequence. Based on the cDNA sequence, the mouse bestrophin protein consists of 551 amino acid residues and has 63% identity and 74% homology to human bestrophin using pair-wise global alignment. The molecular mass of mouse bestrophin is predicted to be approximately 64 kDa with a theoretical isoelectric point (pI) of 8.2. As in humans,[1,4] mouse bestrophin is predicted to be a membrane protein with four transmembrane domains according to a consensus of five different prediction programs. This corresponds well to the four predicted transmembrane domains in human bestrophin.[4]

Developmental Expression of Bestrophin mRNA

To study the expression of bestrophin during development, total RNA was extracted from the eyes of BALBc mice ranging in age from postnatal day (P)1 to adult. RT-PCR was performed, with total RNA used as a template. As shown in Figure 1A, the mouse bestrophin cDNA-specific band was visible throughout postnatal development. Bearing in mind that this is a semiquantitative analysis, the data suggest that bestrophin mRNA expression is strongest in the early postnatal period.

To study more reliably the quantitative expression of bestrophin mRNA we used real-time (*Taq*Man; Applied Biosystems). As shown in Figure 1B, the highest relative expression was detected during early postnatal development (P1–P4), with a constant decline in bestrophin mRNA through adulthood (Fig. 1). During the course of our experiments, no genomic DNA contamination was detected (data not shown).

Biochemical Analysis of Bestrophin Protein Expression

To identify mouse bestrophin, polyclonal antibodies were produced by immunization of rabbits with a peptide derived from the C terminus of mouse bestrophin. The amino acid sequence at the C terminus differs substantially between mouse and human and accounts for the species specificity of antibodies produced using these peptides. We have designated the IgG fraction derived from our polyclonal antisera as Pab-003. To test the function of Pab-003, Western blot was performed on cell lysates from subconfluent RPE-J cells transfected with pEGFP-N1, pcDNA3.1-mbest, or pEGFP-N1-mbest. As shown in Figure 2, Pab-003 detected an ~64-kDa band corresponding to mouse bestrophin in RPE-J cells transfected with pcDNA3.1-mbest. Both Pab-003 and an anti-GFP antibody detected the fused mouse bestrophin+GFP product. The anti-GFP antibody detected GFP produced by the pEGFP-N1 expression vector as well as bestrophin+GFP. When Pab-003 was preincubated with the antigenic peptide, mouse bestrophin was not detected. When Western blot using Pab-003 was performed on lysates derived from the posterior poles of adult mouse eyes, no protein bands were detected (data not shown). Based on our experience with bestrophin in human and porcine eyes,[21,22,29] we presume that our inability to detect mouse bestrophin was probably due to an overall low level of bestro-

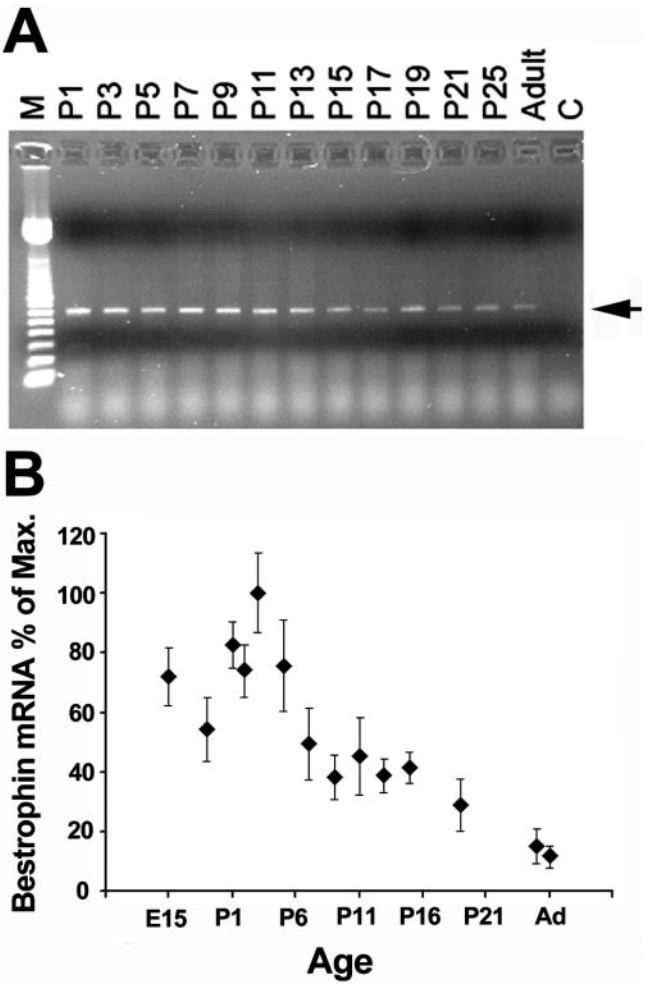

Figure 1. Expression of bestrophin mRNA in mouse eyes during development. (**A**) RT-PCR of total RNA isolated from eyes of mice at postnatal day 1 through 10 weeks. The 626-bp band represents the bestrophin cDNA fragment. *M*: 100-bp ladder; *P1–Adult*: RT-PCR product from mouse eyes of postnatal day 1 through adult (10 weeks); *C*: control RT-PCR with no template. (**B**) Real-time expression of bestrophin mRNA during mouse development using real-time PCR. Expression was detected as early as E15. The highest levels of mRNA expression occurred from P1 to P4 and decreased steadily into adulthood.

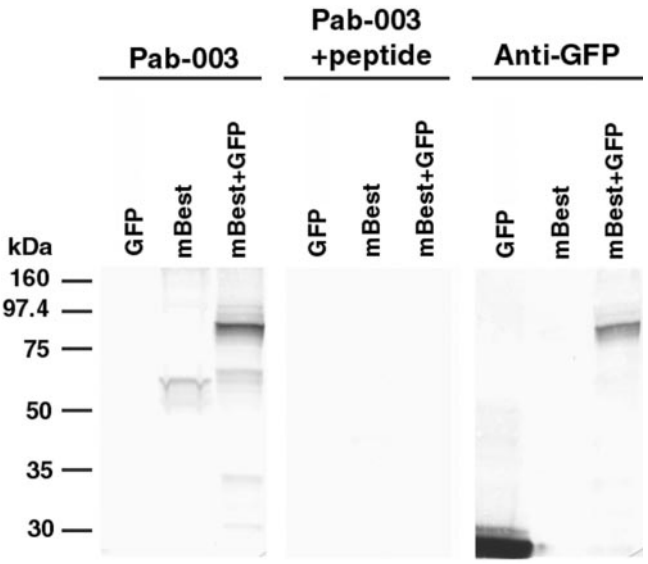

FIGURE 2. Western blot using Pab-003 of RPE-J cells transfected with pEGFP-N1 (GFP), pCDNA3-mBest (mBest), or pEGFP-mBest (mBest+GFP), Pab-003 competed with the antigenic peptide at 100 μg/mL, or an anti-GFP antibody. Note that an ~64-kDa band is identified by Pab-003 in cells transfected with pCDNA3-mBest and the ~93-kDa bestrophin+GFP fusion protein in cells transfected with pEGFP+mBest. No bands were present in cells transfected with pEGFP-N1 or when Pab-003 was preincubated with the antigenic peptide. Anti-GFP antibodies recognized GFP in cells transfected with pEGFP-N1 and also recognized the bestrophin+GFP fusion protein.

phin protein expression in mammalian RPE cells and the comparatively smaller size of mouse eyes.

Immunofluorescenct and Immunohistochemical Analysis of Bestrophin Expression

To determine whether Pab-003 could be used for immunofluorescence and immunohistochemical studies, we first examined the ability of Pab-003 to detect bestrophin in RPE-J cells transfected with pEGFP-N1-mbest. Bestrophin was localized using Pab-003 and the localization compared with that of GFP. Bestrophin and GFP expression were perfectly colocalized (Fig. 3). No staining of nontransfected cells was observed with Pab-003.

To determine the localization of bestrophin protein in the adult eye, we used immunohistochemistry. As shown in Figures 4C and 4D, Pab-003 staining was primarily confined to the basolateral borders of the RPE. This is consistent with the localization of bestrophin as we have reported it in human,[29] monkey,[21] and porcine[21] eyes. In addition, we noted that Pab-003 stained the inner segments of photoreceptors. As a control, Pab-003 was preincubated with a peptide for the antibody epitope. No staining was observed in the RPE or photoreceptors when the antibody was preincubated with the peptide (Figs. 4A, 4B). However, based on in situ hybridization studies in the mouse[1] and our immunohistochemical and biochemical findings in other species[21,29] we conclude that the photoreceptor inner segment staining by Pab-003 is most likely nonspecific.

Because bestrophin expression was too low to detect in adult mice by Western blot, we used immunohistochemistry to observe expression of bestrophin protein during postnatal development. As shown in Figure 5, Pab-003 staining was detected in rudimentary inner segments as early as P1. Because we observed similar nonspecific staining of photoreceptor inner segments in adult eyes (Fig. 4), we believe this to be nonspecific as well. Pab-003 staining of RPE cells did not occur until late in postnatal development. At P10 we consistently observed staining of the basolateral borders of the RPE cells, which was more pronounced at P11.

Electroretinography

The late onset of bestrophin protein expression seemed to correlate with the onset of visual competence of the retina. To examine this further, we performed ERGs on mice to determine the earliest time at which we could detect an ERG a-wave. Figure 6 shows representative ERGs (Fig. 6A) and summary intensity–response functions for the individual ERG components (Fig. 6B–D) obtained from mice aged P9 to P12. Although reproducible responses were not obtained at P9, a clear response was observed from all mice tested at P10. This response comprised an initial cornea-negative a-wave, followed by a small positive b-wave and a later cornea-negative component referred to as slow PIII. Larger amplitude responses were obtained at P11 and P12.

DISCUSSION

In the present study, we defined several basic properties of mouse bestrophin. We first cloned a full-length mouse bestrophin cDNA from a testis cDNA library. Based on sequence analysis, we found mouse bestrophin to be highly similar to the human homologue. Bestrophin mRNA expression was first analyzed with RT-PCR during postnatal development. This revealed an interesting time course of expression with relatively high levels of expression at early postnatal stages and a subsequent decline with age (Fig. 1). In rat, RPE development starts shortly after optic vesicle formation, shown by presence of pigmented cells in the outer layer of retina at E13.5.[30] For this reason, we included embryonic eyes in subsequent studies using quantitative real-time PCR. The real-time PCR experiments confirmed that bestrophin mRNA expression is relatively high during the late phase of embryonic development and early postnatal stages (Fig. 1).

To examine protein expression, we raised a polyclonal antibody (Pab-003) that recognizes mouse bestrophin. Pab-003 was shown to recognize recombinant bestrophin with a high degree of specificity by both immunofluorescence (Fig. 3) and Western blot (Fig. 2). Western blot with Pab-003 on individual mouse eyes did not detect bestrophin. The reason for this is presumably the low level of protein expression and the limited amount of RPE available from a single mouse eye. For one lane in Western blot, one fifth to one tenth of the entire RPE in an eye is needed to detect human bestrophin.[21] To obtain the same amount of isolated RPE from mice would have been impractical. Instead, we used immunohistochemistry to define the developmental time course of bestrophin protein expression.

With Pab-003, bestrophin protein was first detected in the RPE on P10 (Fig. 5). This coincides with other events during eye development. At P10 photoreceptor outer segments are visible,[31] although the eyes are not yet open. Bestrophin has been reported to be a Cl channel,[20] and Sun et al.[20] have proposed that bestrophin generates the Cl^- current that underlies the light peak on EOG or DC-ERG recording. For this reason, we made parallel ERG recordings. Although no reproducible response was observed at P9, we first detected a distinct a-wave at P10, coincident with the appearance of bestrophin in the basolateral plasma membrane of the RPE (Fig. 5). The appearance of the ERG at P10 agrees with prior studies of ERG development.[32–35] At P10, the ERG includes an initial negative a-wave, generated by the light-induced suppression of the photoreceptor dark current.[36] The presence of a cornea-positive b-wave, reflecting activity of bipolar cells,[37,38] indicates that the ribbon synapses already present in the develop-

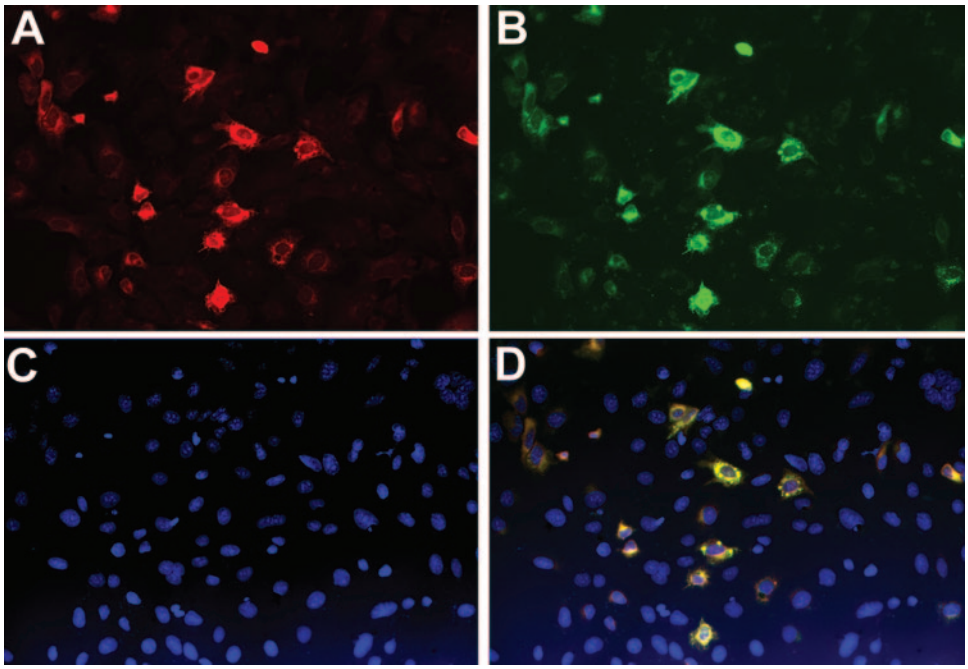

FIGURE 3. Immunofluorescence staining of RPE-J cells transfected with pEGFP-mBest. RPE-J cells were transfected with pEGFP-mBest and stained using Pab-003 with a Texas red–conjugated secondary antibody (**A**, *red*). (**B**) Bestrophin+GFP fluorescence (*green*). (**C**) Cell nuclei stained with DAPI (*blue*). Note the perfect colocalization of Pab-003 and GFP fluorescence indicated by *yellow* in merged images (**D**).

ing outer plexiform layer[39] are functional. The negative polarity component that follows the b-wave is likely to be slow PIII, generated by Kir4.1 channels in retinal glial (Müller) cells.[37] At P11 and P12, the overall amplitude of each ERG component increases, as retinal photoreceptors continue to mature and elaborate their outer segments.[39] Although generation of the a-wave is known to be independent of bestrophin, it can be assumed that the RPE must be capable of reacting to retina-driven electrical events at the onset of visual competence. Although bestrophin is thought to underlie the light peak component of the DC-ERG,[20] we do not have direct evidence that a light peak is generated at these early ages. It is clear, however, that rodents generate a light peak,[40,41] and we plan to examine the developmental time course of the light peak, using a recently developed technique for measuring the mouse dc-ERG (Wu J, Marmorstein AD, Peachey NS, ARVO Abstract 1894, 2003). Nevertheless, the onset of bestrophin

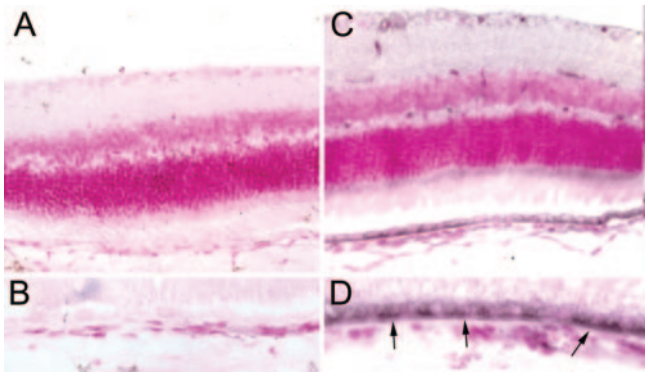

FIGURE 4. Localization of bestrophin in adult mouse eyes. Inspection at low magnification (**A**, **C**) of sections of the posterior pole of mouse eyes indicates bestrophin reactivity (*black*) in the RPE and in photoreceptor inner segments (**C**, **D**), though inner segment staining was most likely due to nonspecific binding of the primary antibody. Inspection at higher magnification (**B**, **D**) reveals that bestrophin staining in the RPE was primarily associated with the basolateral plasma membrane (**D**, *arrows*), consistent with results in other species. (**A**, **B**) Control sections preincubated with the antigenic peptide. Sections were counterstained with nuclear fast red.

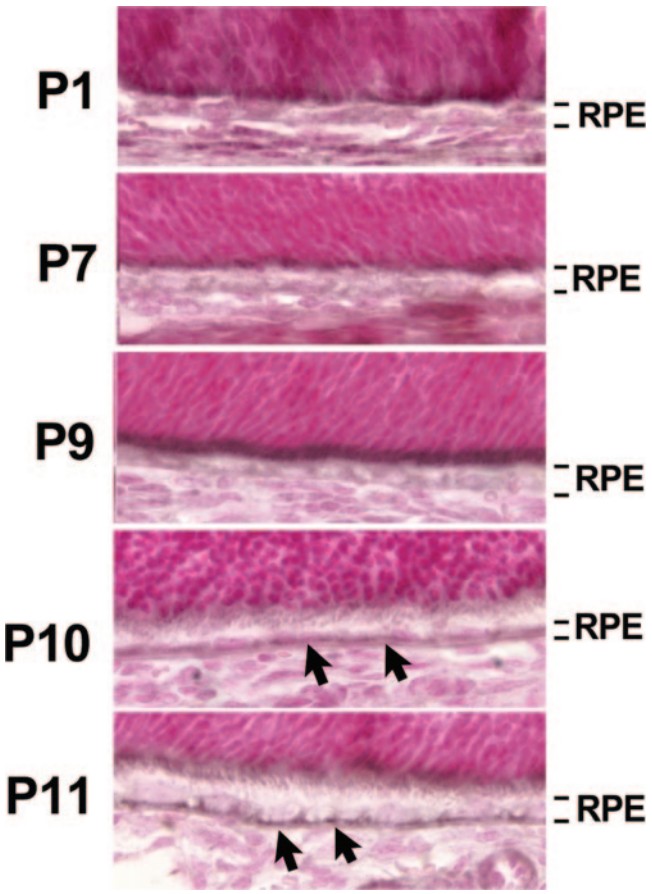

FIGURE 5. Localization of bestrophin in the RPE during mouse postnatal development. Staining of RPE cells was absent from P1 through P9. At P10, a discrete line of bestrophin staining (*arrows*) indicated by a *black* reaction product appeared along the basal membrane of the RPE cells and gained in intensity at P11, discretely outlining the basolateral borders of the RPE.

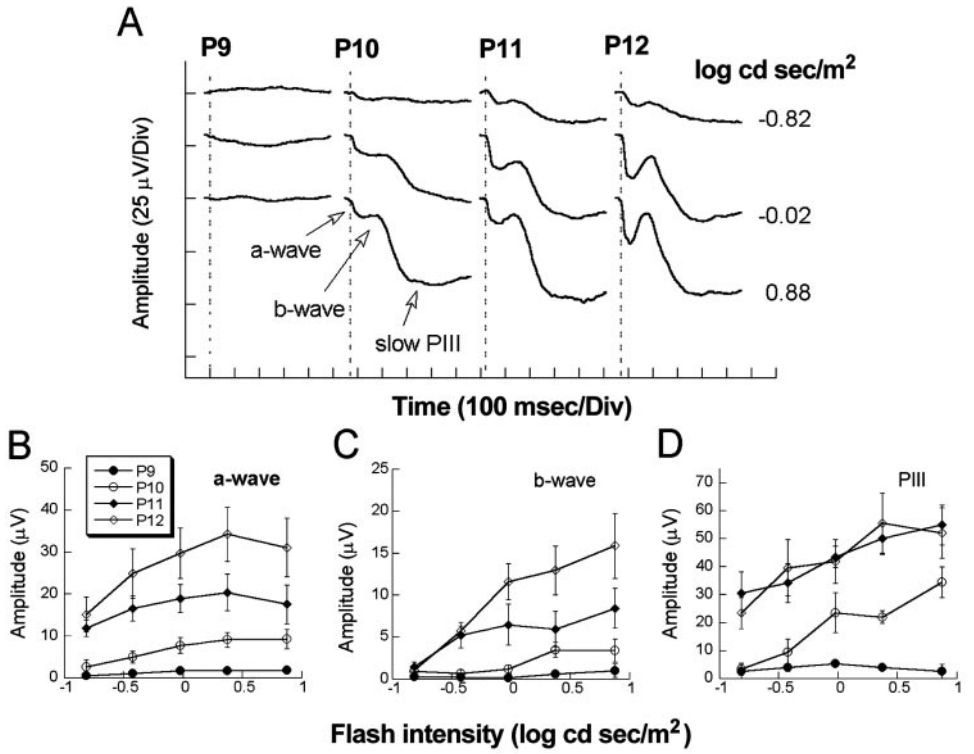

FIGURE 6. Electroretinography. (**A**) Representative ERGs obtained from individual mice tested at the ages indicated. Stimulus intensity ranged from −0.82 to 0.88 log cd-sec/m^2. The *vertical dashed lines* indicate the time of flash presentation and each waveform represents the average response to 25 successive stimuli presented with a 5.1-second interstimulus interval. The major components of the response are indicated for the P10 response to a 0.88 log cd-sec/m^2 stimulus. (**B–D**) Amplitude of the different ERG components plotted as a function of flash intensity: (**B**) a-wave; (**C**) b-wave; (**D**) slow PIII. Each data point indicates the average of results in four to seven mice; error bars ± 1 SEM.

expression at P10 is compatible with the hypothesis that bestrophin plays a role in generating or regulating the RPE response to retinal activity, a process in which the light peak is likely to be involved.

The present results indicate that bestrophin protein is an excellent marker for RPE differentiation. The definition of differentiation in RPE cell culture systems is highly variable. Maintenance of RPE-specific functions, such as visual cycle and phagocytosis, and the expression of genes and proteins associated with these functions are measures that have typically been applied to cell lines. In many studies, however, changes in gene expression pattern of a limited set of markers have been used as the criteria for differentiation. Typically these markers include cellular retinaldehyde-binding protein (CRALBP) and RPE65, both of which are involved in the visual cycle. CRALBP protein is expressed from birth in the RPE,[42] Müller cells,[42] brain, and optic nerve.[43] RPE65 is expressed only in RPE cells[44] and cone photoreceptors.[45] Although RPE65 mRNA is present, even in embryonic eyes,[46] based on immunohistochemistry in rat, RPE65 protein expression begins at P4.[46] A later marker for RPE differentiation is β5-integrin, which is involved in phagocytosis of photoreceptor outer segments and was detected by Western blot at P7 in rat.[47] We have examined expression of bestrophin mRNA and protein in three RPE-derived cell lines.[21] Although all three expressed bestrophin mRNA, none of those cells expressed bestrophin protein.[21] In fact, only one RPE culture model has been reported to produce bestrophin protein.[48] This model also exhibits many other properties of RPE cells, including polarized Cl^- transport[49] and probably represents the most differentiated culture model currently available. From these data, it is clear that the maturation of the RPE occurs gradually with different RPE-specific processes coming online at different time points in development. A more comprehensive knowledge of differences in gene and protein expression patterns will allow us to be more precise in our definition of RPE differentiation in the laboratory. Competence to respond to photoreceptor activity may be the last RPE-specific process to occur developmentally.

In summary, we have found that the onset of bestrophin protein expression is coincident with the visual competence of photoreceptors and that the onset of expression of bestrophin mRNA and protein in the mouse RPE is significantly different. These data should be taken as an indicator that gene expression analysis of RPE-derived cultures as a means of determining level of differentiation may be very misleading.

Acknowledgments

The authors thank Jessica Giancola, Nichole Kyle, Precious J. McLaughlin, Eric Pennock, and J. Brett Stanton for excellent technical assistance.

References

1. Petrukhin K, Koisti MJ, Bakall B, et al. Identification of the gene responsible for Best macular dystrophy. *Nat Genet.* 1998;19:241–247.
2. Marquardt A, Stohr H, Passmore LA, Kramer F, Rivera A, Weber BH. Mutations in a novel gene, VMD2, encoding a protein of unknown properties cause juvenile-onset vitelliform macular dystrophy (Best's disease). *Hum Mol Genet.* 1998;7:1517–1525.
3. Allikmets R, Seddon JM, Bernstein PS, et al. Evaluation of the Best disease gene in patients with age-related macular degeneration and other maculopathies. *Hum Genet.* 1999;104:449–453.
4. Bakall B, Marknell T, Ingvast S, et al. The mutation spectrum of the bestrophin protein–functional implications. *Hum Genet.* 1999; 104:383–389.
5. Caldwell GM, Kakuk LE, Griesinger IB, et al. Bestrophin gene mutations in patients with Best vitelliform macular dystrophy. *Genomics* 1999;58:98–101.
6. Eksandh L, Bakall B, Bauer B, Wadelius C, Andreasson S. Best's vitelliform macular dystrophy caused by a new mutation (Val89Ala) in the VMD2 gene. *Ophthalmic Genet.* 2001;22:107–115.
7. Kramer F, White K, Pauleikhoff D, et al. Mutations in the VMD2 gene are associated with juvenile-onset vitelliform macular dystrophy (Best disease) and adult vitelliform macular dystrophy but not age-related macular degeneration. *Eur J Hum Genet.* 2000;8:286–292.

8. Lotery AJ, Munier FL, Fishman GA, et al. Allelic variation in the VMD2 gene in best disease and age-related macular degeneration. *Invest Ophthalmol Vis Sci.* 2000;41:1291–1296.
9. Marchant D, Gogat K, Boutboul S, et al. Identification of novel VMD2 gene mutations in patients with best vitelliform macular dystrophy. *Hum Mutat.* 2001;17:235.
10. Palomba G, Rozzo C, Angius A, Pierrottet CO, Orzalesi N, Pirastu M. A novel spontaneous missense mutation in VMD2 gene is a cause of a Best macular dystrophy sporadic case. *Am J Ophthalmol.* 2000;129:260–262.
11. Marchant D, Gogat K, Dureau P, et al. Use of denaturing HPLC and automated sequencing to screen the VMD2 gene for mutations associated with Best's vitelliform macular dystrophy. *Ophthalmic Genet.* 2002;23:167–174.
12. Yanagi Y, Sekine H, Mori M. Identification of a novel VMD2 mutation in Japanese patients with Best disease. *Ophthalmic Genet.* 2002;23:129–133.
13. Cross HE, Bard L. Electro-oculography in Best's muscular dystrophy. *Am J Ophthalmol.* 1974;77:46–50.
14. Gass JDM. *Stereoscopic Atlas of Macular Diseases*: *Diagnosis and Treatment*. St. Louis: Mosby; 1997.
15. Maloney WF, Robertson DM, Duboff S M. Hereditary vitelliform macular degeneration: variable fundus findings within a single pedigree. *Arch Ophthalmol.* 1977;95:979–983.
16. Bard LA, Cross HE. Genetic counseling of families with Best macular dystrophy. *Trans Am Acad Ophthalmol Otolaryngol.* 1975; 79:OP865–OP873.
17. Gallemore RP, Hughes BA, Miller SS. Light-induced responses of the retinal pigment epithelium. In: Marmor MF, Wolfsenberger TJ, eds. *The Retinal Pigment Epithelium*: *Function and Disease.* New York: Oxford University Press; 1998:175–198.
18. Gallemore RP, Steinberg RH. Effects of DIDS on the chick retinal pigment epithelium. II. Mechanism of the light peak and other responses originating at the basal membrane. *J Neurosci.* 1989;9: 1977–1984.
19. Gallemore RP, Steinberg RH. Light-evoked modulation of basolateral membrane Cl− conductance in chick retinal pigment epithelium: the light peak and fast oscillation. *J Neurophysiol.* 1993;70:1669–1680.
20. Sun H, Tsunenari T, Yau KW, Nathans J. The vitelliform macular dystrophy protein defines a new family of chloride channels. *Proc Natl Acad Sci USA.* 2002;99:4008–4013.
21. Marmorstein AD, Marmorstein LY, Rayborn M, Wang X, Hollyfield JG, Petrukhin K. Bestrophin, the product of the Best vitelliform macular dystrophy gene (VMD2), localizes to the basolateral plasma membrane of the retinal pigment epithelium. *Proc Natl Acad Sci USA.* 2000;97:12758–12763.
22. Marmorstein LY, McLaughlin PJ, Stanton JB, Yan L, Crabb JW, Marmorstein AD. Bestrophin interacts physically and functionally with protein phosphatase 2A. *J Biol Chem.* 2002;277:30591–30597.
23. Stohr H, Marquardt A, Nanda I, Schmid M, Weber BH. Three novel human VMD2-like genes are members of the evolutionary highly conserved RFP-TM family. *Eur J Hum Genet.* 2002;10:281–284.
24. Walter G, Scheidtmann, KH, Carbone A, Laudano AP, Doolittle R F. Antibodies specific for the carboxy- and amino-terminal regions of simian virus 40 large tumor antigen. *Proc Natl Acad Sci USA.* 1980;77:5197–5200.
25. Marmorstein AD, Gan YC, Bonilha VL, Finnemann SC, Csaky KG, Rodriguez-Boulan E. Apical polarity of N-CAM and EMMPRIN in retinal pigment epithelium resulting from suppression of basolateral signal recognition. *J Cell Biol.* 1998;142:697–710.
26. Marmorstein LY, Ouchi T, Aaronson SA. The BRCA2 gene product functionally interacts with p53 and RAD51. *Proc Natl Acad Sci USA.* 1998;95:13869–13874.
27. Marmorstein LY, Kinev AV, Chan GK, et al. A human BRCA2 complex containing a structural DNA binding component influences cell cycle progression. *Cell.* 2001;104:247–257.
28. Marmorstein LY, Munier FL, Arsenijevic Y, et al. Aberrant accumulation of EFEMP1 underlies drusen formation in Malattia Leventinese and age-related macular degeneration. *Proc Natl Acad Sci USA.* 2002;99:13067–13072.
29. Hoppe G, Marmorstein LY, Marmorstein AD. Localization and functional analysis of bestrophin, In: Anderson RE, LaVail MM, Hollyfield JG, eds. *New Insights into Retinal Degeneration Diseases.* New York: Kluwer Academic/Plenum Publishers; 2001: 207–216.
30. Kuwabara T, Weidman TA. Development of the prenatal rat retina. *Invest Ophthalmol.* 1974;13:725–739.
31. Smith RS, Kao WW-Y, John SWM. Ocular development, In: Smith RS, ed. *Systematic Evaluation of the Mouse Eye.* Boca Raton, FL: CRC Press; 2002:45–63.
32. Keeler CE, Sutcliffe E, Chaffee EL. A description of the ontogenetic development of retinal action currents in the house mouse. *Proc Natl Acad Sci USA.* 1928;14:811–815.
33. Noell W. Differentiation, metabolic organization and viability of the visual cell. *Arch Ophthalmol.* 1958;60:702–733.
34. Rohrer B, Korenbrot JI, LaVail MM, Reichardt LF, Xu B. Role of neurotrophin receptor TrkB in the maturation of rod photoreceptors and establishment of synaptic transmission to the inner retina. *J Neurosci.* 1999;19:8919–8930.
35. Jaissle GB, May CA, Reinhard J, et al. Evaluation of the rhodopsin knockout mouse as a model of pure cone function. *Invest Ophthalmol Vis Sci.* 2001;42:506–513.
36. Lamb TD. Gain and kinetics of activation in the G-protein cascade of phototransduction. *Proc Natl Acad Sci USA.* 1996;93:566–570.
37. Kofuji P, Ceelen P, Zahs KR, Surbeck LW, Lester HA, Newman EA. Genetic inactivation of an inwardly rectifying potassium channel (Kir4.1 subunit) in mice: phenotypic impact in retina. *J Neurosci.* 2000;20:5733–5740.
38. Robson JG, Frishman LJ. Response linearity and kinetics of the cat retina: the bipolar cell component of the dark-adapted electroretinogram. *Vis Neurosci.* 1995;12:837–850.
39. Olney JW. An electron microscopic study of synapse formation, receptor outer segment development, and other aspects of developing mouse retina. *Invest Ophthalmol.* 1968;7:250–268.
40. Kikawada N. Variations in the corneo-retinal standing potential of the vertebrate eye during light and dark adaptations. *Jpn J Physiol.* 1968;18:687–702.
41. Peachey NS, Stanton JB, Marmorstein AD. Noninvasive recording and response characteristics of the rat dc-electroretinogram. *Vis Neurosci.* 2002;19:693–701.
42. Eisenfeld AJ, Bunt-Milam AH, Saari JC. Localization of retinoid-binding proteins in developing rat retina. *Exp Eye Res.* 1985;41: 299–304.
43. Saari JC, Huang J, Possin DE, et al. Cellular retinaldehyde-binding protein is expressed by oligodendrocytes in optic nerve and brain. *Glia.* 1997;21:259–268.
44. Hamel CP, Tsilou E, Harris E, et al. A developmentally regulated microsomal protein specific for the pigment epithelium of the vertebrate retina. *J Neurosci Res.* 1993;34:414–425.
45. Znoiko SL, Crouch RK, Moiseyev G, Ma JX. Identification of the RPE65 protein in mammalian cone photoreceptors. *Invest Ophthalmol Vis Sci.* 2002;43:1604–1609.
46. Manes G, Leducq R, Kucharczak J, Pages A, Schmitt-Bernard CF, Hamel CP. Rat messenger RNA for the retinal pigment epithelium-specific protein RPE65 gradually accumulates in two weeks from late embryonic days. *FEBS Lett.* 1998;423:133–137.
47. Finnemann SC, Bonilha VL, Marmorstein AD, Rodriguez-Boulan E. Phagocytosis of rod outer segments by retinal pigment epithelial cells requires alpha(v)beta5 integrin for binding but not for internalization. *Proc Natl Acad Sci USA.* 1997;94:12932–12937.
48. Hu J, Bok D. A cell culture medium that supports the differentiation of human retinal pigment epithelium into functionally polarized monolayers. *Mol Vis.* 2001;7:14–19.
49. Hu JG, Gallemore RP, Bok D, Frambach DA. Chloride transport in cultured fetal human retinal pigment epithelium. *Exp Eye Res.* 1996;62:443–448.